Journal of Sound and Vibration (1997) **207**(3), 351–364

OPTIMAL ACTIVE SUSPENSION DESIGN USING CONSTRAINED OPTIMIZATION

A. ZAREMBA

Automated Analysis Corporation, 2805 *South Industrial*, *Suite* 100, *Ann Arbor*, *Michigan* 48104-6767, *U.S.A.*

AND

R. HAMPO AND D. HROVAT

Ford Motor Company, *P.O. Box* 2053, *MD* 1170-*SRL*, *Dearborn*, *Michigan* 49121-2053, *U.S.A.*

(*Received* 5 *August* 1996, *and in final form* 5 *May* 1997)

In a quarter-car vehicle model, optimal control schemes for an active suspension are designed using a constrained optimization procedure. The control laws obtained minimize the H_2-norm of vehicle acceleration subject to constraints on r.m.s. values of the suspension stroke, tire deformation and actuator force. Constraints imposed on feedback coefficients define quasi-optimal control laws that show increased robustness to system parameter variations and disturbances. To impact body acceleration at frequencies near the unsprung mass mode, tire damping is introduced in the model. The optimal and quasi-optimal control schemes were partially verified on a quarter-car simulator with a random road input and the preliminary results are encouraging. The tests showed significant improvement (3–5 dB) of body acceleration response in the frequency range up to 25 Hz and increased robustness of the quasi-optimal control laws, that use lower amounts of spring cancellation.

1. INTRODUCTION

The synthesis of active suspensions for advanced automotive applications aimed to improve the ride comfort and handling properties of vehicles has been a topic of vigorous research during the past two or three decades [1–13].

In early studies [1, 3] attention was given to the advantages of "skyhook" damping which put damping in the system at sprung mass frequency ω_s (where $\omega_s^2 = k_s/m_s$, k_s being the suspension spring rate and m_s the sprung mass) without deteriorating high frequency performance.

The synthesis for a one-DOF quarter-car model is presented in reference [2] using optimal filtering based on the Wiener–Höpf approach. In reference [5], the sprung mass jerk is included in the model as an additional comfort measure. The design of an optimal suspension based on a two-DOF quarter-car model is performed in references [6, 8] and [2]. The results of the global study are presented in the form of "carpet" plots parameterized in terms of the performance index weights.

Alternative control laws for active suspensions are evaluated in reference [9], with the emphasis on the LQG compensator using suspension deflection as the measurement. The robustness of the LQ/H_2 controller to uncertainties in the passive suspension elements for some ride regimes has been established in reference [12]. Some related aspects of the

0022–460X/97/430351 + 14 $25.00/0/sv971117

dynamics, optimal and adaptive control of vibrating and elastic systems were considered in references [14–17].

In this paper a novel approach is presented to synthesizing an active suspension using a constrained optimization procedure. We minimize a performance index which represents r.m.s. passenger acceleration while r.m.s. suspension deflection and also r.m.s. tire deformation are considered explicitly as constraints imposed on the system. This approach does not require tuning the weighting parameters and obtains the best ride quality for given suspension rattle space and road holding parameters. In addition, r.m.s. actuator force and feedback coefficients can be also constrained.

The main advantage of the proposed method is that the desired optimal solution, satisfying the required constraints, is now obtained explicitly. However, the associated numerics are now more involved than in the conventional *LQG* case, since the proposed method is based on general non-linear programming. In view of this, it can be said that the two methods nicely complement each other. The *LQG* approach can be used in the first phase to obtain the global overview of all the possible optimal solutions. The proposed method could then be used to determine a specific optimal solution, using the above global map as a basis for determining an initial, meaningful constraint set. Further refinements of the solution would then be possible with the proposed method, which can accept many additional constraints not suitable for the conventional *LQG* setting.

We design the following optimal control laws: a full state feedback; a partial state feedback (excluding the term that is proportional to the tire deflection); and a control scheme that contains the integral of the suspension deflection. The integral term was introduced in reference [4] to eliminate the steady state position offset caused by external force disturbances. It also appeared in reference [5] as the result of minimizing a jerk in the performance index.

Constraints imposed on the feedback gains define quasi-optimal control laws which employ less than optimal spring cancellation, η (where $\eta = |C_1|/k_s$ and C_1 is the gain that is proportional to suspension deflection). The quasi-optimal control laws increase the effective stiffness of the system in comparison with the optimal feedback and make the plant less sensitive to system parameter variations and disturbances.

The analysis also showed the importance of accounting for tire damping in the model. Tire damping couples the sprung and unsprung mass motions that affect passenger acceleration at the wheelhop frequency, ω_u (where $\omega_u^2 = k_t/m_u$, m_u being the unsprung mass and k_t the tire spring rate) [10].

The results of optimization are compared in the case of the full state feedback with the corresponding *LQG* design. It is demonstrated, for a number of operational points, that the discepancy in the optimal ride quality (r.m.s. vehicle acceleration) between the two methods is less than 1% and is within the accuracy of numerical calculations.

The paper is organized as follows. In section 2 the suspension design problem is formulated as an optimization problem with constraints. The results of optimization are presented in section 3, with the preliminary test results based on a quarter-car hardware simulator with random road input being summarized in section 4. Concluding remarks are given in section 5.

2. VEHICLE DYNAMIC MODEL AND PROBLEM STATEMENT

We consider a quarter-car vehicle model (Figure 1) that is described by the vector equation

$$\dot{x} = Ax + \Gamma \dot{z}_r + Bu. \tag{1}$$

Here u is the control input, x is the vector of state variables, such that

$$x_1 = z_s - z_u, \qquad x_2 = \dot{z}_s, \qquad x_3 = z_u - z_r, \qquad x_4 = \dot{z}_u, \tag{2}$$

where x_1 and x_3 are suspension and tire deflections from equilibrium position, and x_2 and x_4 are sprung and unsprung mass velocities, respectively.

In equation (1), matrices A, B and Γ are defined as

$$A = \begin{bmatrix} 0 & 1 & 0 & -1 \\ -\omega_s^2 & -2\xi_s\omega_s & 0 & 2\xi_s\omega_s \\ 0 & 0 & 0 & 1 \\ \rho\omega_s^2 & 2\rho\xi_s\omega_s & -\omega_u^2 & -2\rho\xi_s\omega_s - 2\xi_u\omega_u \end{bmatrix}, \qquad \Gamma = \begin{bmatrix} 0 \\ 0 \\ -1 \\ 2\xi_u\omega_u \end{bmatrix},$$

$$B = \begin{bmatrix} 0 \\ 1/m_s \\ 0 \\ -\rho/m_s \end{bmatrix}, \tag{3}$$

where $\omega_s = (k_s/m_s)^{1/2}$, $\omega_u = (k_t/m_u)^{1/2}$, $\rho = m_s/m_u$, $\xi_u = b_t/2(m_u k_t)^{1/2}$, $\xi_s = b_s/2(m_s k_s)^{1/2}$ and $\dot{z}_r$ represents the road roughness disturbance velocity input modelled as a white-noise process, specified by

$$\mathrm{E}[\dot{z}_r(t)] = 0, \qquad \mathrm{E}[\dot{z}_r(t_1), \dot{z}_r(t_2)] = 2\pi A V \delta(t_1 - t_2). \tag{4, 5}$$

In equations (4) and (5), E denotes the expectation and $\delta(\cdot)$ represents the Dirac function, with A and V being the road roughness factor and the vehicle speed, respectively.

The tire damping is included in the model (1)–(3). It was shown in reference [10] that taking tire damping to be small but non-zero couples the motion of the sprung and unsprung masses at all frequencies, and allows reduction of the passenger acceleration at frequencies near the wheelhop mode ω_u.

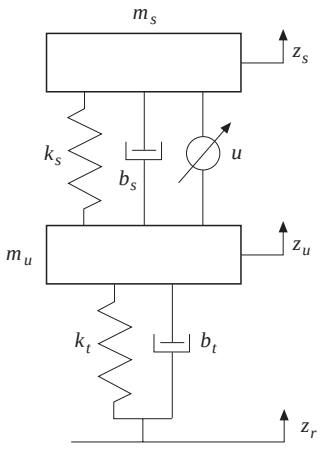

Figure 1. A quarter-car model with active suspension: m_s = sprung mass, b_s = suspension damping, k_s = suspension spring rate, m_u = unsprung mass, k_t = tire stiffness, b_t = tire damping, u = actuator force, z_r = road displacement, z_u = unsprung mass displacement, z_s = sprung mass displacement.

We define the following transfer functions

$$H_A(s) = \frac{\ddot{z}_s(s)}{\dot{z}_r(s)}, \qquad H_{RS}(s) = \frac{z_s(s) - z_u(s)}{\dot{z}_r(s)},$$

$$H_{TD}(s) = \frac{z_u(s) - z_r(s)}{\dot{z}_r(s)}, \qquad H_u(s) = \frac{u}{\dot{z}_r(s)}, \tag{6}$$

as the sprung mass acceleration, suspension deflection, tire deflection and actuator force transfer functions, respectively.

Henceforth, we investigate feedback control laws which, in their most general form, contain an integral term

$$u = -\sum_{i=1}^{4} C_i x_i - C_5 \int_0^t x_1(\tau)\, \mathrm{d}\tau. \tag{7}$$

Introducing the integral term in equation (7) eliminates steady state position offset caused by external disturbances and improves the high frequency NVH isolation [4, 5].

It is straightforward to obtain analytical expressions for transfer function (6) using the dynamic model (1)–(3) and feedback control laws (7). In Appendix A, the transfer functions (6) are derived for the case of full state feedback ($C_5 = 0$ in equation (7)). Transfer functions for the general form control laws (7), accounting for an integral term, are given in Appendix B. In Appendix C asymptotic properties of transfer functions are analyzed and comparisons are given for the cases of a passive suspension, an active suspension with full state feedback control ($C_i = 0$ in equation (7)), and an active suspension with control including an integral term.

Space H_2 is defined as a space of functions which are square integrable on the imaginary axis and analytic in the open right-half plane with the norm

$$\|F\|_2 = \left(1/2\pi \int_{-\infty}^{\infty} F(\mathrm{j}\omega) F^*(\mathrm{j}\omega)\, \mathrm{d}\omega \right)^{1/2}. \tag{8}$$

For the dynamic systems (1)–(3) with random input (4) and (5), the norm (8) of the transfer functions (6) represents root mean square (r.m.s.) values of sprung mass acceleration, suspension deflection, tire deflection and actuator force, respectively.

One can also evoke [5]

$$\mathrm{E}[y^2] = 1/2\pi S_0 \int_{-\infty}^{\infty} |H(\omega)|^2\, \mathrm{d}\omega, \tag{9}$$

where $S_0 = 2\pi AV$ is a spectral density of the input $\dot{z}_r$, y is the system output and H is the corresponding transfer function.

Combining the formulas (8) and (9), we obtain the r.m.s. values of sprung mass acceleration, suspension deflection, tire deflection and actuator force:

$$H_A^{rms} = S_0^{1/2} \|H_A\|_2, \qquad H_{RS}^{rms} = S_0^{1/2} \|H_{RS}\|_2, \qquad H_{TD}^{rms} = S_0^{1/2} \|H_{TD}\|_2, \qquad H_u^{rms} = S_0^{1/2} \|H_u\|_2.$$

The optimal control design problem can now be formulated as follows: given a dynamic system (1)–(3) and control law (7), find optimal feedback coefficients from the convex set $C \in \Omega$, $C = (C_1, \ldots, C_5)^{\mathrm{t}}$ minimizing the $\|H_A\|_2$-norm subject to constraints on the r.m.s. values of the suspension deflection, the tire deformation and the actuator force:

$$\min \{ \|H_A\|_2 : C \in \Omega \text{ such that } H_{RS}^{rms} \leqslant h_r, H_{TD}^{rms} \leqslant h_c, H_u^{rms} \leqslant h_u \}. \tag{10}$$

The optimal control solution of equation (10) provides the best ride quality (in the sense of the above H_2-norm) for the given suspension package, road holding and the actuator force constraints.

3. OPTIMAL CONTROL SYNTHESIS

To obtain a solution of the optimal control problem (10) we use a $MATRIX_x$ optimization module [18]. It solves the general non-linear programming problem

$$\min_p F(p), \tag{11}$$

subject to

$$G(p) = 0, \qquad h_l \leqslant H(p) \leqslant h_u, \qquad p_l \leqslant p \leqslant p_u. \tag{12–14}$$

The optimization procedure parameters were selected as

$$R = 10^{-4}, \qquad \delta_p = 10^{-6}, \qquad \delta_t = 10^{-8},$$

where R is the penalty parameter for controlling the search for a feasible region, δ_p is the perturbation parameter for numerical gradient computation and δ_t is the tolerance on optimality and feasibility [18]. The value of penalty parameter greater than one forces the search to stay close to the known feasible range; a smaller value of R allows a broader range of searching.

The cost function for optimization was selected as

$$\Phi = k \| H_A \|_2, \tag{15}$$

where scalar k was varied in the limits $k = 10^8$–10^{12}. Use of the scaling coefficient k improves the accuracy of the optimization.

The relevant parameters for an illustrative example used for the optimization procedure are

$$\rho = 5{\cdot}86, \qquad f_s = 1{\cdot}49 \text{ Hz}, \qquad f_u = 8{\cdot}27 \text{ Hz}, \qquad \xi_s = 0{\cdot}11, \qquad \xi_u = 0{\cdot}017.$$

To evaluate the precision of the proposed method, the results of constrained optimization can be compared in the case of the full state feedback with the corresponding LQG problem solution [11]. Solving the LQG problem given weighting factors r_1 and r_2 in the performance index, we calculated the r.m.s. vehicle acceleration u_{LQG}^{rms}, the r.m.s. suspension stroke X_{1LQG}^{rms} and the r.m.s tire deformation X_{3LQG}^{rms}. The optimal r.m.s. suspension stroke X_{1LQG}^{rms} and r.m.s. tire deformation X_{3LQG}^{rms} values were then used as constraints for numerical optimization. It was shown for several operational points that typical differences between the optimal solution (r.m.s. vehicle acceleration H_A^{rms}) determined from the above numerical optimization and the corresponding LQG optimal value u_{LQG}^{rms} are less than 1%:

$$\frac{|H_A^{rms} - u_{LQG}^{rms}|}{u_{LQG}^{rms}} < 0{\cdot}01.$$

This is a function of the number of iterations and the accuracy of the numerical calculations.

The results of numerical optimization are shown in Figures 2 and 3. Optimal body acceleration versus road velocity transfer functions are plotted for different constraints on suspension packaging and road holding. Note that, due to non-zero unsprung damping, there is now significant variability between these curves, even around the wheelhop frequency, at which, ideally for $\xi_u = 0$, one should have an invariant point.

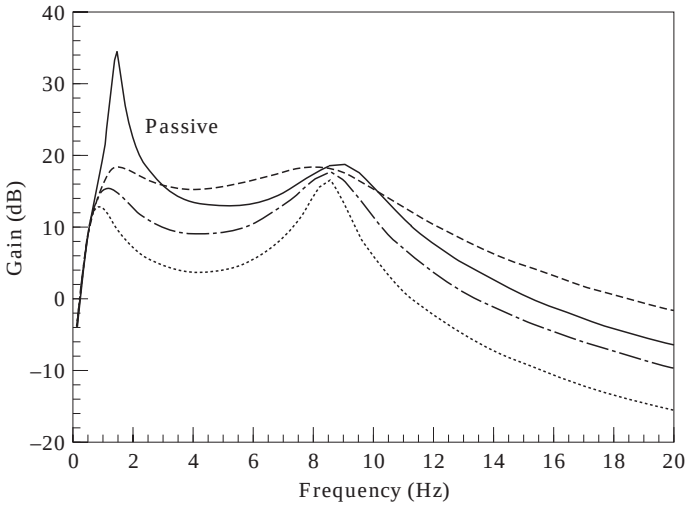

Figure 2. Optimal body acceleration transfer functions ——, Passive suspension body accceleration transfer functions; ----, optimal body acceleration transfer function for experiment 1 in Table 1; –·–·–, optimal body acceleration transfer function for experiment 3 in Table 1; · · · · · , optimal body acceleration transfer function for experiment 5 in Table 1.

We investigate control laws (7) while setting to zero the tire deflection term (i.e., $C_3 = 0$), since the tire deflection is difficult to measure.

In Table 1 are presented the optimal normalized r.m.s. body acceleration value $\tilde{J}_a^{opt}$, the optimal feedback coefficients and normalized r.m.s. values of suspension rattle space and tire deformation constraints $\tilde{h}_r^{rms}$ and $\tilde{h}_c^{rms}$. Optimal body acceleration versus road velocity transfer functions for experiments 1, 3 and 5 in Table 1 are given in Figure 1.

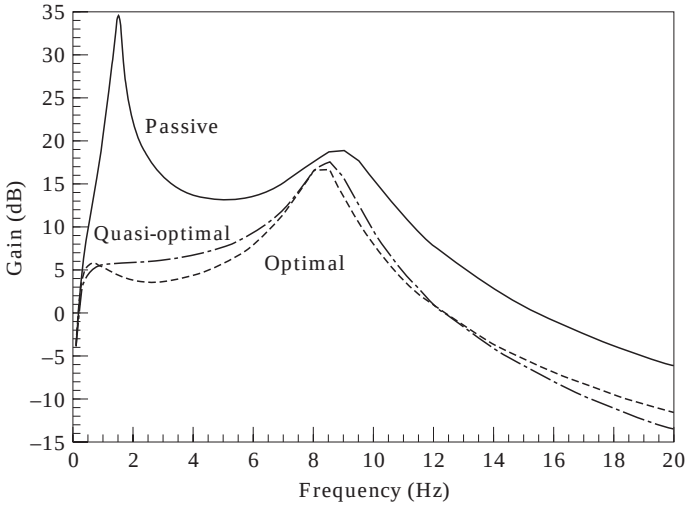

Figure 3. Optimal and quasi-optimal body acceleration transfer functions: ——, Passive suspension body acceleration transfer function; –·–·–, quasi-optimal body acceleration transfer function for typical rattle space and tire deformation constraints $\tilde{h}_r = 0{\cdot}56$, $\tilde{h}_c = 0{\cdot}23$ and additional constraint on spring cancellation $C_1 > 0$; ----, optimal body acceleration transfer function for typical rattle space and tire deformation constraints $\tilde{h}_r = 0{\cdot}56$ and $\tilde{h}_c = 0{\cdot}23$.

TABLE 1

Optimal suspension design for control laws without tire deformation term ($C_3 = 0$), *without the integral term* ($C_5 = 0$) *and for different suspension deflection constraints* ($\tilde{h}_r^{rms}$) *and minimal tire deformation constraints* ($\tilde{h}_c^{rms}$)

Number	$\tilde{J}_a^{opt}$	$\tilde{h}_r^{rms}$	$\tilde{h}_c^{rms}$	C_1	C_2	C_4
1	32·6	0·3	0·15	−5 199	3390	−760
2	21·2	0·4	0·2	−16 718	2430	223
3	14·4	0·5	0·26	−25 087	1460	524
4	9·85	0·6	0·34	−29 115	869	668
5	6·58	0·7	0·4	−31 331	464	745
6	4·24	0·8	0·46	−32 700	171	786
7	2·7	0·9	0·5	−33 548	−44	807

Numerical calculations showed that the rattle space and tire deformation constraints are closely related. Any value of one constraint corresponds to a narrow range of the other constraint where the performance measure could be improved. Given a rattle space constraint ($\tilde{h}_r^{rms}$), Table 1 contains the lower bound of the corresponding tire deformation constraint ($\tilde{h}_c^{rms}$). Increasing values of constraints imposed on the system improves the body acceleration peformance and results in higher spring cancellation in the optimal control law (Table 1).

Numerical calculations and prior experience [12] also showed that control laws with high spring cancellation are sensitive to system parameter variations. Next, in Figure 3 and Table 2 are presented results for optimization under typical rattle space and tire deformation constraints $\tilde{h}_r = 0{\cdot}56$ and $\tilde{h}_c = 0{\cdot}23$, and with different constraints on spring cancellation. In Figure 3 are shown optimal body acceleration transfer functions, while Table 2 contains results of the optimization when imposing additional constraints on feedback coefficient C_1 to confine the spring cancellation. System eigenvalues for optimal and quasi-optimal suspension design are presented in Table 2. For completeness, optimization results for the control without integral term ($C_5 = 0$), with the same constraints on spring cancellation as in Table 2, are presented in Table C2 (Appendix C).

Varying spring cancellation from the optimal value to zero results in increasing the optimal performance index by only $\delta J_a^{opt} = 11\%$. From Table 2 it follows that damping terms and an integral term are increased when decreasing the spring cancellation. The last line in the table defines a quasi-optimal control law that needs only damping terms and an integral for implementation.

TABLE 2

Optimal suspension design for control with integral term under rattle space and tire deformation constraints of $\tilde{h}_r^{rms} = 0{\cdot}56$ *and* $\tilde{h}_c^{rms} = 0{\cdot}23$, *and with different constraints on spring cancellation*

η (%)	$\tilde{J}_a^{opt}$	C_1	C_2	C_4	C_5	$E_{1,2}$	E_3	E_4	E_5
85·7	15·22	−29 877	1 990	346	729	−4·4 ± 52j	−3·59	−3·22	−0·16
74·3	15·23	−25 936	4 693	372	2522	−4·3 ± 52j	−11·8	−1·5	−0·35
57·1	15·26	−19 995	7 280	408	2420	−4·3 ± 53j	−17·6	−1·87	−0·18
28·6	15·99	−9 999	12 480	511	4128	−4·2 ± 53j	−29·4	−1·82	−0·18
0	16·99	1	18 286	532	5874	−4·6 ± 53j	−42·8	−1·72	−0·19

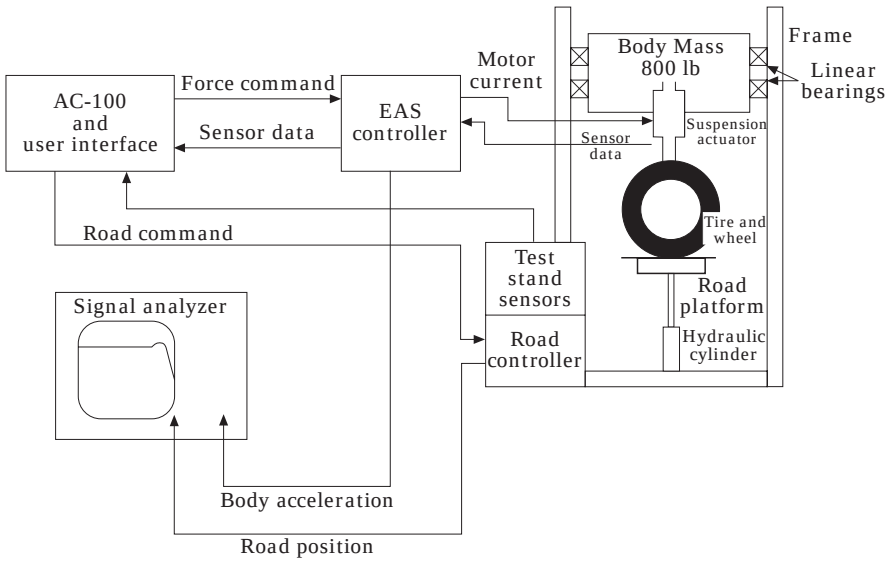

Figure 4. The optimal control test set-up: a block-diagram of the single wheel test stand.

4. CONTROL LAWS EVALUATION

The optimal control development and testing were carried out using a single wheel test stand, in the form of a quarter-car laboratory simulator shown in Figure 4.

The active suspension linear actuator [19] used in this investigation is powered by a permanent magnet synchronous motor. This actuator is positioned between the vehicle body and a suspension control arm so as to provide a controlled force between the body and wheel. The motor is a rotary design, with the rotary to linear force conversion accomplished via a ballscrew/ballnut combination. The rotor of the motor is attached directly to the ballscrew. As torque is generated by the motor, the torque is converted to linear force by the ballscrew/ballnut. The motor is controlled by a solid state inverter which synthesizes the proper motor phase current waveforms required to produce the commanded torque.

The actuator used has the ability to produce up to 6200 N of force at velocities up to 1.5 m/s. In order to reduce the average power required, a parallel spring was used to support the static vehicle weight. The system was designed to be energy efficient, requiring no standby power draw, unlike conventional hydraulic active suspension systems.

Conventional tuning of control parameters proceeded in three steps. First, simulations were performed and the control gains adjusted to provide good response over simulated road surfaces. Next, the single-wheel test stand was used to verify and further tune the gains. This test stand simulated different road surfaces using a hydraulic cylinder to move the road surface vertically. The last step of tuning was performed in the test vehicle on the road. Many road surfaces were driven over and performance measurements calculated for each of these tests. Generally, on-road performance was very similar to that of the single wheel test stand. This validation proved the value of the single wheel test stand, in that it allowed easier and more consistent parameter adjustment.

The system measurements included body acceleration, wheel acceleration, and spring deflection. The accelerations were numerically integrated and processed to yield velocities. The AC-100 rapid development system tool was used and set up so that the optimal gains could be adjusted from the computer screen. A HP control systems analyzer was used to

measure the transfer function of the whole system, from road position input to body acceleration output, using the optimal outer loop control laws.

In Figure 5 are presented body acceleration versus displacement transfer functions obtained by using (1) previously developed, empirically (trial-and-error) based control (curve 1), (2) optimal control (7) with $\eta = 85\%$ spring cancellation (curve 2), and (3) quasi-optimal control with zero spring cancellation $\eta = 0$ (curve 3). Tests showed improvement of the body acceleration response for optimal and quasi-optimal (3–5 dB) control laws in the frequency range up to 25 Hz. From Figure 5 it seems that the plant has two regions in which the three curves are relatively close. Note that the first region appears at a frequency of about 11–12 Hz (the linear model that we used for optimization has a resonance around 9 Hz). This is primarily due to non-linear tire properties. First, this discrepancy shows the limitations of a linear tire model. Second, it demonstrates the robustness of our method that offers increased performance in spite of modelling inaccuracy.

The second region appears around 18 Hz as a result of vibrations of the test stand in the vertical plane. This mode has not been included in the model. Also, at low frequencies up to 1 Hz the system response is contaminated by additional noise and low frequency test stand vibrations.

Although the experimental results do not correlate completely with analytical results due to non-linearities and unmodelled dynamics, they show that the method is robust and can improve immediately the system which was tuned previously by trial and error.

The test results also indicate that the performance of the quasi-optimal control laws for the particular case considered here was better than the optimal. It is believed that this is the result of improved robustness with respect to system modelling inaccuracies handled by the quasi-optimal control.

5. CONCLUSIONS

An optimization procedure has been developed for optimal active suspension design that minimizes r.m.s. body acceleration while r.m.s. suspension deflection, as well as tire deformation, are considered as constraints imposed on the system. This approach offers an alternative to the weighting-parameter tuning, and directly obtains the best ride quality (in the sense of the H_2-norm) for given suspension packaging and holding parameters.

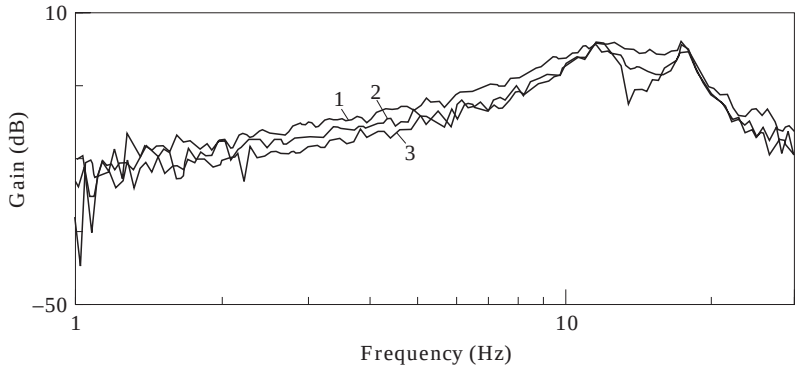

Figure 5. The body acceleration/road displacement transfer function. 1, measured for passive suspension; 2, measured for optimal suspension design (first line in Table 2); 3, measured for quasi-optimal suspension design (last line in Table 2).

Accounting for constraints on feedback coefficients defines quasi-optimal control laws with less spring cancellation, that show promise for increased robustness to system parameter variations and disturbances. This will be the subject of further study.

The asymptotic analysis of system transfer functions allows the determination of conditions which result in improving the high frequency performance of the plant.

The procedure can be modified to accont for realistic road inputs, real actuator performance limitations and also non-linear properties of suspension elements.

ACKNOWLEDGMENTS

The authors would like to gratefully acknowledge constructive discussions with colleagues at Ford; Ross Stuntz, John Miller, Roy Davis and others.

REFERENCES

1. E. K. Bender 1967 *ScD thesis*, *Massachusetts Institute of Technology*, *Cambridge*, *Massachusetts*. Optimization of the random vibration characteristics of vehicle suspensions using random process theory.
2. E. K. Bender 1967 *Proceedings of JACC*, 135–143. Optimum linear control of random vibrations.
3. J. K. Hedrick and D. N. Wormley 1975 *Transactions of the American Society of Mechanical Engineers*, *Monograph*, *Mechanical of Transportation Systems*, *AMD* **15**. Active suspension for ground transport vehicles—a state of the art review.
4. C. M. Harris and C. E. Crede 1976 *Shock and Vibration Handbook*. New York: McGraw-Hill.
5. D. Hrovat and M. Hubbard 1981 *Transactions of the American Society of Mechanical Engineers*, *Journal of Dynamic Systems*, *Measurement*, *and Control* **103**, 228–236. Optimum vehicle suspension minimizing RMS rattlespace, sprung-mass acceleration and jerk.
6. D. Hrovat 1984 *Ford Motor Company Internal Document and Presentation*, *Dearborn*, *Michigan*, 15 March. Performance tradeoffs for an LQG-optimal suspension.
7. R. M. Chalasani 1986 *Transactions of the American Society of Mechanical Engineers Monograph*, *AMD* **80**, *DSC* **2**, 187–204. Ride performance potential of active suspension systems—part I.
8. D. Hrovat 1987 *Ford Motor Company Research Report*, Dearborn, Michigan, September. Influence of unsprung weight on vehicle ride quality. Also, *Journal of Sound and Vibration* **124**, 497–516.
9. C. Yue, T. Butsuen and J. K. Hedrick 1989 *Transactions of the American Society of Mechanical Engineers*, *Journal of Dynamic Systems*, *Measurement*, *and Control* **111**, 286–291. Alternative control laws for automotive active suspensions.
10. J. A. Levit and N. G. Zorka 1991 *Transactions of the American Society of Mechanical Engineers*, *Journal of Dynamic Systems*, *Measurement*, *and Control* **113**, 134–137. The influence of tire damping in quarter car active suspension models.
11. D. Hrovat 1993 *Transactions of the American Society of Mechanical Engineers*, *Journal of Dynamic Systems*, *Measurement*, *and Control* **115**, 328–342. Applications of optimal control to advanced automotive suspension design.
12. A. G. Ulsoy, D. Hrovat and T. Tseng 1996 *Transactions of the American Society of Mechanical Engineers*, *Journal of Dynamic Systems*, *Measurement*, *and Control* **116**, 123–131. Stability robustness of LQ and LQG active suspensions.
13. A. T. Zaremba, R. Hampo and D. Hrovat 1994 *International Symposium on Advanced Vehicle Control*, *Japan*. Control synthesis for an automotive active suspension using constrained optimization.
14. A. L. Fradkov and A. T. Zaremba 1992 18*th International Congress of Theoretical and Applied Mechanics*, *Haifa*. Dynamics, optimal and speed-gradient adaptive control of flexible robotic manipulators.
15. A. T. Zaremba and R. I. Davis 1995 *Proceedings of Amer. Contr. Conference*, 4253–4257. Dynamic analysis and stability of a power assist steering system.
16. A. T. Zaremba 1996 *Dynamics and Control* **6**, 179–198. Adaptive control of flexible link manipulators using a pseudolink dynamic model.

17. A. T. Zaremba 1997 *Applied Mathematics and Mechanics* **61**, 37–43. Stabilization of programmed motions of a rigid body under uncertainties of a dynamic model.
18. *MATRIX$_x$*, Integrated Systems Inc., 101 University Avenue, Palo Alto, California 94301-1695, U.S.A.
19. R. I. Davis and P. B. Patil 1992 *US Patent* 5,060,959 (issued 29 October). Electrically powered active suspension for a vehicle.

APPENDIX A: TRANSFER FUNCTIONS FOR FULL STATE FEEDBACK

Equations (1)–(3) can be written in the form

$$m_s\ddot{z}_s = k_s(z_u - z_s) + b_s(\dot{z}_u - \dot{z}_s) + u, \tag{A1}$$

$$m_u\ddot{z}_u = -k_s(z_u - z_s) - b_s(\dot{z}_u - \dot{z}_s) - u + k_t(z_r - z_u) + b_t(\dot{z}_r - \dot{z}_u). \tag{A2}$$

By adding equations (A1) and (A2) we find that

$$m_s\ddot{z}_s + m_u\ddot{z}_u = k_t(z_r - z_u) + b_t(\dot{z}_r - \dot{z}_u). \tag{A3}$$

Transforming equation (A3) with zero initial conditions, we obtain

$$z_u(s) = \frac{(k_t + sb_t)z_r - m_s s^2 z_s}{s^2 m_u + sb_t + k_t}, \tag{A4}$$

where $s = j\omega$. Substituting equation (A4) into equation (A1) and using control law (7) yields

$$\Delta(s)z_s = d_a(s)z_r, \tag{A5}$$

where

$$\Delta(s) = m_u m_s s^4 + [m_u(b_s + C_2) + m_s(b_t + b_s - C_4)]s^3 + [(k_s + C_1)m_u + (k_t + k_s + C_1 - C_3)m_s + (C_2 + b_s)b_t]s^2 + [(b_s + C_2)k_t + b_t(C_1 + k_s)]s + (k_s + C_1)k_t, \tag{A6}$$

$$d_a(s) = s^2(b_s b_t + C_3 m_u - C_4 b_t) + s[(k_s + C_1)b_t + k_t(b_s - C_4)] + k_t(k_s + C_1). \tag{A7}$$

Using equation (A5), we determine that

$$H_A(s) = s\, d_a(s)/\Delta(s). \tag{A8}$$

From equation (A3), we also find that

$$z_s(s) = \frac{-(m_u s^2 + b_t s + k_t)z_u + (b_t s + k_t)z_r}{m_s s^2}. \tag{A9}$$

Substituting equation (A9) into equation (A2) yields

$$\Delta(s)z_u = d_u(s)z_r, \tag{A10}$$

where

$$d_u(s) = m_s b_t s^3 + s^2[b_t(C_2 + b_s) + m_s(k_t - C_3)] + s[b_t(k_s + C_1) + k_t(b_s + C_2)] + k_t(C_1 + k_s). \tag{A11}$$

Now we can obtain the rattle space transfer function

$$H_{RS}(s) = \frac{d_a(s) - d_u(s)}{\Delta(s)s} = \frac{-s^2 m_s b_t + s[m_u C_3 - (C_2 + C_4)b_t - m_s(k_t - C_3)] - k_t(C_2 + C_4)}{\Delta(s)} \tag{A12}$$

and the road holding transfer function

$$H_{TD}(s) = \frac{d_u(s) - \Delta(s)}{\Delta(s)s}$$
$$= \frac{-s^3 m_s m_u + s^2[m_u(b_s + C_2) + m_s(b_s - C_4)] - s(k_s + C_1)(m_u + m_s)}{\Delta(s)}. \quad \text{(A13)}$$

Using equations (7), (A5), (A10), (A12) and (A13), the transfer function for the actuator force is calculated as follows:

$$H_u(s) = -C_1 H_{RS}(s) - C_2 \frac{d_a(s)}{\Delta(s)} - C_3 H_{TD}(s) - C_4 \frac{d_u(s)}{\Delta(s)}. \quad \text{(A14)}$$

APPENDIX B: TRANSFER FUNCTIONS FOR CONTROL WITH INTEGRAL TERM

Accounting for the integral term in the control law given by equation (8), we find that

$$\Delta^I(s) z_s(s) = d_a^I(s) z_r, \qquad \Delta^I(s) z_u(s) = d_u^I(s) z_r, \quad \text{(B1, B2)}$$

where

$$d_a^I(s) = s d_a(s) + C_5(k_t + s b_t), \qquad d_u^I(s) = s d_u(s) + C_5(k_t + s b_t),$$
$$\Delta^I(s) = s\Delta(s) + C_5[(m_u + m_s)s^2 + b_t s + k_t]. \quad \text{(B3)}$$

Here, $d_a(s)$, $d_u(s)$ and $\Delta(s)$ are determined in Appendix A.

Using equations (B1)–(B3), we find expressions for transfer functions:

$$H_A^I(s) = s \frac{d_a^I(s)}{\Delta^I(s)}, \qquad H_{RS}^I(s) = \frac{s\Delta(s)}{\Delta^I(s)} H_{RS}(s), \quad \text{(B4, B5)}$$

$$H_{TD}^I(s) = \frac{d_u(s) - \Delta(s) - sC_5(m_u + m_s)}{\Delta^I(s)}, \quad \text{(B6)}$$

$$H_u^I(s) = -(C_1 + 1/sC_5) H_{RS}^I(s) - C_2 \frac{d_a^I(s)}{\Delta^I(s)} - C_3 H_{TD}^I(s) - C_4 \frac{d_u^I(s)}{\Delta^I(s)}. \quad \text{(B7)}$$

Setting $C_5 = 0$ in expressions for transfer functions (B1)–(B7) makes them coincide with formulas obtained in Appendix A.

APPENDIX C: ASYMPTOTIC ANALYSIS OF TRANSFER FUNCTIONS

The body acceleration transfer functions can be approximated at low frequencies as

$$H_A(s),\ H_A^I(s),\ H_A^P(s) = s + o(s), \quad \text{(C1)}$$

where

$$\lim_{s \to 0} o(s)/s = 0.$$

The high frequency asymptotes can be written as

$$H_A(s),\ H_A^I(s) = \frac{b_s b_t + C_3 m_u - C_4 b_t}{m_u m_s} \frac{1}{s} + o\left(\frac{1}{s}\right). \quad \text{(C2)}$$

From equations (C1) and (C2), it follows that acceleration asymptotes are independent of the integral term.

Setting $f = 0$ ($C_3 = 0$, $C_4 = 0$) in equation (C2), we find the passive system high frequency acceleration asymptote:

$$H_A^p(s) = \frac{b_s b_t}{m_u m_s}\frac{1}{s} + o\left(\frac{1}{s}\right). \tag{C3}$$

By proper choice of feedback coefficients in equation (C2),

$$b_s b_t + C_3 m_u - C_4 b_t = 0, \tag{C4}$$

the active system could improve the high frequency performance of the plant when compared to the passive system (C3):

$$H_A(s),\ H_A^I(s) = \frac{(k_s + C_1)b_t + k_t(b_s - C_4)}{m_u m_s}\frac{1}{s^2} + o\left(\frac{1}{s^2}\right). \tag{C5}$$

Since tire deformation would be hard to measure, for control laws with $C_3 = 0$, equation (C4) means that the tire damping coefficient C_4 should compensate for the suspension damping $C_4 = b_s$.

Asymptotic analysis results (C4) and (C5) differ from the results obtained in reference [9] due the presence of the tire damping term b_t in the dynamic model.

Using equations (A6), (A7), (A11), (A12), (B3) and (B5), we find the high and low frequency suspension deformation asymptotes:

$$H_{RS}(s),\ H_{RS}^I(s),\ H_{RS}^P(s) = -\frac{b_t}{m_u}\frac{1}{s^2} + o\left(\frac{1}{s^2}\right), \tag{C6}$$

$$H_{RS}^P(s) = -s\frac{m_s}{k_s} + o(s), \qquad H_{RS}(s) = -\frac{C_2 + C_4}{k_s + C_1} + o(s), \tag{C7, C8}$$

$$H_{RS}^I(s) = -s\frac{C_2 + C_4}{C_5} + o(s). \tag{C9}$$

From equation (C9) it follows that a suspension design with an integral term has a better low frequency rattle space asymptote in comparison to control with $C_5 = 0$ that has a finite dc gain (C8).

The tire deformation asymptotes are

$$H_{TD}(s),\ H_{TD}^I(s),\ H_{TD}^P(s) = -\frac{1}{s} + o\left(\frac{1}{s}\right), \tag{C10}$$

$$H_{TD}(s),\ H_{TD}^I(s),\ H_{TD}^P(s) = -s\frac{m_u + m_s}{k_t} + o(s), \tag{C11}$$

and from equations (A14) and (B7) we find the actuator force asymptotes:

$$H_u(s) = -\frac{k_s(C_2 + C_4)}{k_s + c_1} + o(s),\ H_u^I = o(s), \tag{C12}$$

$$H_u(s),\ H_u^I(s) = \left(-C_3 + C_4\frac{b_t}{m_u}\right)\frac{1}{s} + o\left(\frac{1}{s}\right). \tag{C13}$$

TABLE C1

Asymptotic properties of transfer functions for passive suspension (PS), *active suspension* (AS), *and active suspension with integral term* (IT)

Transfer function	PS	AS	AS with IT
$H_{A\,s\to 0}$	s	s	s
$H_{A\,s\to\infty}$	$\dfrac{b_s b_t}{m_u m_s}\dfrac{1}{s}$	$\dfrac{b_s b_t + C_3 m_u - C_4 b_t}{m_u m_s}\dfrac{1}{s}$	$\dfrac{b_s b_t + C_3 m_u - C_4 b_t}{m_u m_s}\dfrac{1}{s}$
if $b_s b_t + C_3 m_u - C_4 b_t = 0$		$\dfrac{(k_s + C_1) b_t + k_t (b_s - C_4)}{m_u m_s}\dfrac{1}{s^2}$	$\dfrac{(k_s + C_1) b_t + k_t (b_s - C_4)}{m_u m_s}\dfrac{1}{s^2}$
$H_{RS\,s\to 0}$	$-s\, m_s/k_s$	$-\dfrac{C_2 + C_4}{k_s + C_1}$	$-s\dfrac{C_2 + C_4}{C_5}$
$H_{RS\,s\to\infty}$	$-\dfrac{b_t}{m_u}\dfrac{1}{s^2}$	$-\dfrac{b_t}{m_u}\dfrac{1}{s^2}$	$-\dfrac{b_t}{m_u}\dfrac{1}{s^2}$
$H_{TD\,s\to 0}$	$-s\dfrac{m_u + m_s}{k_t}$	$-s\dfrac{m_u + m_s}{k_t}$	$-s\dfrac{m_u + m_s}{k_t}$
$H_{TD\,s\to\infty}$	$-\dfrac{1}{s}$	$-\dfrac{1}{s}$	$-\dfrac{1}{s}$
$H_{u\,s\to 0}$	–	$-\dfrac{k_s (C_2 + C_4)}{k_s + C_1}$	0
$H_{u\,s\to\infty}$	–	$-\left(C_3 + C_4\dfrac{b_t}{m_u}\right)\dfrac{1}{s}$	$-\left(C_3 + C_4\dfrac{b_t}{m_u}\right)\dfrac{1}{s}$

TABLE C2

Optimal suspension design for control laws without the tire deformation term ($C_3 = 0$), *without the integral term* ($C_5 = 0$) *and with different constraints on spring cancellation*

η (%)	$\tilde{J}_a^{opt}$	C_1	C_2	C_4	$E_{1,2}$	E_3	E_4
85·7	15·81	−28 645	2 660	316	−4.65 ± 52j	−6·0	−2·62
74·3	15·83	−25 977	4 019	329	−4·61 ± 52j	−9·6	−2·31
57·1	15·93	−19 994	7 034	370	−4·53 ± 52j	−16·9	−2·16
28·6	16·42	−9 998	11 987	469	−4·42 ± 53j	−28·2	−2·1
0	17·42	4	17 229	531	−4·7 ± 5.73j	−39·9	−2·1

Equation (C12) shows that the integral term improves the actuator low frequency asymptote as well as the rattle space low frequency performance. The results of asymptotic analysis are summarized in Table C1. In Table C2 are shown results of optimization for the control without the integral term ($C_5 = 0$), with the same constraints on spring cancellation as in Table 2.